CHARACTERIZING SELF-FORMING LIPID BILAYERS IN LOW-VOLTAGE ELECTROWETTING SYSTEMS

A thesis

submitted by

Ingrid Guha

In partial fulfillment of the requirements

for the degree of

Master of Science

in

Mechanical Engineering

TUFTS UNIVERSITY

May 2012

ADVISER:

Prof. Behrouz Abedian

DISCLAIMER

This work was performed at MIT Lincoln Laboratory and was supported in part by the U.S. Air Force under Contract No. FA8721-05-C002. Opinions, interpretations, conclusions, and recommendations are those of the author and are not necessarily endorsed by the United States Government.

ABSTRACT

This thesis reports the first-time demonstration of lipid bilayers as reversibly wettable dielectrics in electrowetting systems and characterizes various physical and electrical properties of lipid bilayers, with the aim of assessing the capabilities and limitations of using these thin liquid films in electrowetting-powered microfluidic devices. Lipid bilayers enable high contact angle changes at lower voltages than alternative organic dielectrics in electrowetting systems, reducing the required voltage by approximately an order of magnitude. Thus, lipid bilayers offer a promising approach to developing low-voltage, low power-consumption electrowetting devices. This thesis characterizes the electrowetting behavior of systems containing lipid bilayers (e.g. contact angle as a function of voltage), as well as other physical and electrical properties, including lipid bilayer thickness in response to applied electrostatic pressure, lipid bilayer conductivity under applied electric fields, and changes in lipid bilayer thickness with respect to time between voltage transitions. A discussion on the morphology of lipid bilayers formed from two oil-based surfactants, sorbitan monooleate (Span 80) and sorbitan trioleate (Span 85), is presented.

ACKNOWLEDGMENTS

This thesis was supported by a DARPA-MIT Lincoln Laboratory Research Assistantship through the Advanced Silicon Technology Group at MIT Lincoln Laboratory. I would like to acknowledge Dr. Shaun Berry for his helpful guidance with my research and thesis writing, Professor Behrouz Abedian for his mentoring and guidance during my graduate school career, and especially Dr. Jakub Kedzierski, for his invaluable advice, encouragement, and support.

TABLE OF CONTENTS **PAGE**

LIST OF TABLES

LIST OF FIGURES

INTRODUCTION

1.1 Introduction to electrowetting

Electrowetting alters the contact angle of a liquid drop on a solid surface via voltage application across the solid-liquid interface. This phenomenon provides a general means of converting electrical energy to mechanical energy. The typical electrowetting configuration consists of a conductive liquid drop (often water-based) on a dielectric stack covering a planar electrode, as shown in Figure 1. The Lippmann-Young equation, derived from thermodynamic considerations on the phenomenon of electrowetting, can be used to predict the contact angle change in response to voltage [1]:

$$cos\theta = cos\theta_Y + \frac{CV^2}{2\gamma_{wo}} \tag{1}$$

where θ is the contact angle of the water drop as a function of voltage, θ_Y is the angle at zero voltage (known as Young's angle), C is the capacitance per area of the dielectric, V is the voltage applied between the electrode and the water drop, and γ_{WO} is the surface energy between the water and the nonconductive ambient phase, commonly air or oil. Experimental measurements of the water contact angle with respect to applied voltage in a variety of electrowetting systems generally align with the Lippman-Young equation.

As the applied voltage increases, the contact angle that the water drop forms at the interface with the solid surface continually decreases until the contact angle reaches a fundamental lower limit, known as the saturation point. Beyond this limit, the contact angle ceases to decrease despite an increase in voltage. Virtually all electrowetting systems exhibit contact angle saturation; however, the saturation point for any given electrowetting system is highly materials-dependent and proves challenging to predict. A consensus has not yet been reached as to precise mechanism of contact angle saturation, though several theories to date have been proposed [2, 3, 4].

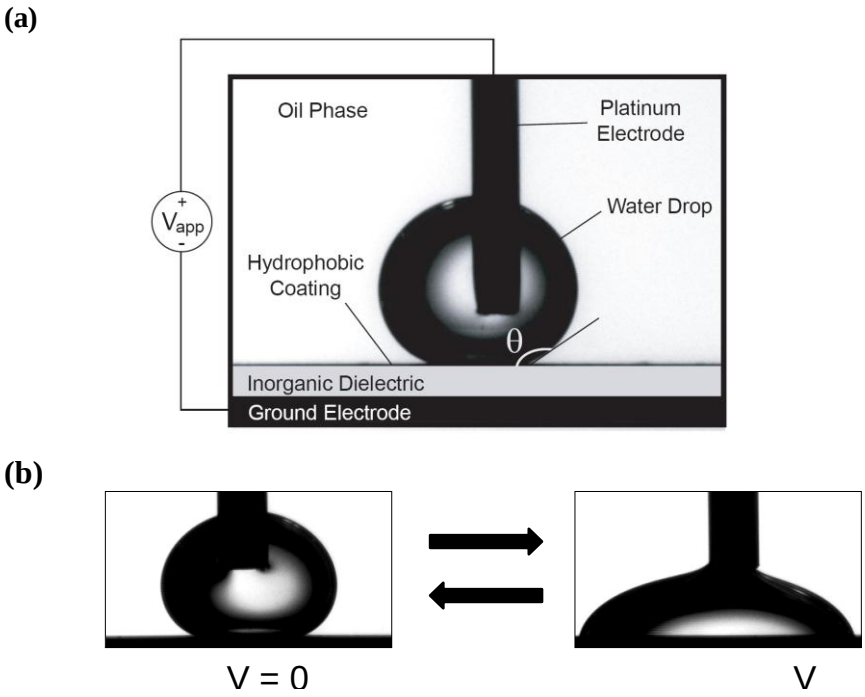

Figure 1. (a) Representative electrowetting configuration. The solid surface consists of three layers from bottom to top: a doped silicon layer (ground electrode), an inorganic dielectric layer, and a hydrophobic coating. A water drop containing electrolytes and/or surfactants is placed on the hydrophobic coating, and the entire setup is immersed in a non-conductive oil medium. A voltage is applied across an inorganic dielectric layer and the hydrophobic coating to decrease the contact angle (θ). The voltage application lowers the surface energy between the water drop and the solid surface, consequently decreasing θ. (b) Effect of electrowetting a water drop. At zero voltage, the water drop rests on a hydrophobic surface with a high contact angle. When a voltage is applied, the water drop wets the surface. The drop returns to its original conformation when the voltage is removed again.

1.2 Lipid bilayers in electrowetting systems

Electrowetting finds use in a variety of microfluidic applications, including liquid displays [5, 6, 7], liquid lenses [8, 9, 10], and miniaturized bioassays [11, 12]. Virtually all electrowetting systems used in research studies or for commercial applications rely on spin-coated amorphous fluoropolymers, such as Teflon AF™ or Cytop™, on top of inorganic dielectrics to obtain reversible wetting [13, 14, 15]. Although fluoropolymers enable reversible wetting, their electrical properties—low permittivities and low

breakdown fields—render them poor dielectrics [16, 17]. Electrical breakdown of the fluoropolymer irreparably damages the electrowetting properties of the system, even if the inorganic dielectrics beneath the fluoropolymer remain intact. Thick fluoropolymer films are required to reduce the electric field and prevent dielectric breakdown of the fluoropolymer, resulting in high actuation voltages for electrowetting, typically exceeding 10 V [1, 18]. Lipid bilayers display improved electrical properties over fluoropolymers that enable a drastic reduction in the voltage required for electrowetting. This thesis will explore various properties of lipid bilayers in electrowetting systems to assess the capabilities of this alternative dielectric layer.

The development of reliable, low-voltage electrowetting systems is essential for realizing portable, battery-powered electrowetting devices. Compared to fluoropolymers, lipid bilayers exhibit higher capacitances per area and higher breakdown fields, facilitating high contact angle changes at low voltages in electrowetting systems comparable to those observed in mercury/oil/water electrocapillary systems without dielectric layers [19]. Lipid bilayers enable reversible electrowetting with minimal contact angle hysteresis, so that the contact angle changes consistently and predictably in response to the applied voltage, without dependence on previously applied voltages across the same dielectric surface. Lipid bilayers also exhibit interesting liquid dielectric properties, such as pressure-dependent thickness and some ability to self-heal after electrical damage. Interestingly, the electrowetting effect only works in systems containing lipid bilayers with AC voltages at frequencies around 50 Hz and above. However, at sufficiently high frequencies, lipid bilayers offer a promising approach to the development of reliable, low-voltage electrowetting systems for use in portable electrowetting devices.

1.3 Formation of stable lipid bilayers

Lipid bilayers form spontaneously between water drops and hafnium oxide surfaces from appropriate oil-based surfactants at sufficiently high concentrations, via adsorption of the surfactant from

the oil phase onto the oil-hafnium oxide and oil-water interfaces, as depicted in Figure 2. The disjoining pressure between the two layers of adsorbed surfactant maintains physical separation between the water drop and hafnium oxide surface. Even during electrowetting, there remains a thin oil layer between the water drop and the hafnium oxide surface. Surfactant bilayers are commonly used to stabilize water-in-oil emulsions [20, 21] and have even been used to electrowet two water drops against each other [22]. However, this effect has never before been exploited for reversible electrowetting of a water drop on a solid, hydrophilic dielectric surface. In these types of electrowetting systems, stable lipid bilayers may be formed using non-ionic, lipophilic surfactants. This thesis focuses on lipid bilayers formed from two such surfactants: sorbitan monooleate (Span 80) and sorbitan trioleate (Span 85). Table 1 provides the molecular weights and chemical structures of these surfactants.

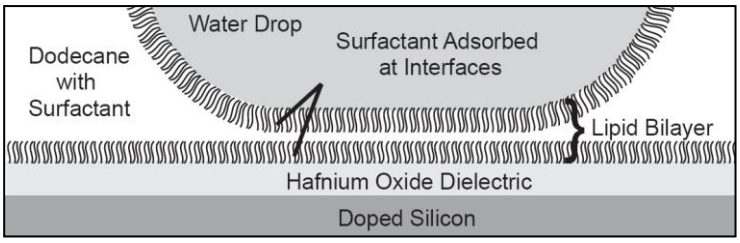

Figure 2. Schematic drawing of a lipid bilayer formed from a surfactant dissolved in dodecane. The surfactant adsorbs at the oil-hafnium oxide and oil-water interfaces, forming a thin oil-based lipid bilayer that buffers the water drop from the hafnium oxide surface.

Table 1. Molecular weights and chemical structures of Span 80 and Span 85, both of which may be used to form lipid bilayers on hafnium oxide in electrowetting systems.

Surfactant Name	**Molecular weight (g/mol)**	**Chemical Structure** [23]
Span 80 (sorbitan monooleate)	**428.6**	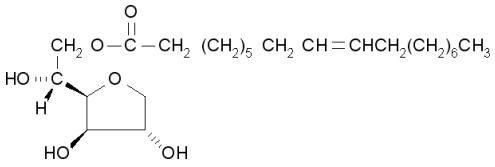
Span 85 (sorbitan trioleate)	**957.5**	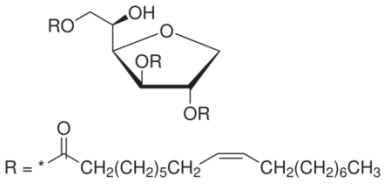

As shown in Table 1, Span 80 and Span 85 are amphipathic surfactants that contain a hydrophilic head and 1 and 3 lipid tails, respectively, with one carbon-carbon double bond per tail. All these surfactants are liquid at room temperature; the double bond in the hydrocarbon tails may give rise to disorder within the surfactant, inducing liquidity at room temperature and the self-healing properties observed in lipid bilayers formed from these surfactants. Similarly structured surfactants without carbon-carbon double bonds (e.g. Span 60, Span 65) do not form stable lipid bilayers in electrowetting systems. In the presence of these surfactants, water drops irreversibly wet hafnium oxide surfaces in otherwise identical environments.

For a stable lipid bilayer to form between a water drop and a hafnium oxide surface, there must be a minimum concentration of surfactant present in the oil ambient. The minimum required concentration is different for each surfactant, and presumably depends on the base oil as well, though only dodecane was used to experiment with the formation of stable lipid bilayers. In the case of Span 85, only

~0.8 mM is needed to form a stable lipid bilayer. Span 80 must be present at a concentration of ~2 mM in dodecane to form a stable lipid bilayer. The concentrations of surfactant required to form a lipid bilayer generally produce low oil-water surface energies (<4 mJ/m^2) in these electrowetting systems, consequently reducing the speed of electrowetting effects as well as the voltage required to induce a given contact angle change.

When forming a stable lipid bilayer, the water drop must be dispensed onto the hafnium oxide in oil. If the water drop is first placed on hafnium oxide in air and then submersed in oil, the water drop remains pinned to the surface with a hydrophilic contact angle, though the contact angle slowly increases over the following days. This steady increase suggests that the formation of the lipid bilayer is a thermodynamically stable process, and that direct contact between the water drop and the hafnium oxide surface in dodecane with these surfactants is therefore not stable over long timescales.

Interestingly, water drops containing fluorosurfactants do not exhibit reversible wetting in systems with lipid bilayers. Water drops containing fluorinated surfactants irreversibly wet hafnium oxide surfaces, whereas water drops containing non-fluorinated surfactants show complete wetting reversibility. (Approximately ten non-fluorinated surfactants and three fluorinated water-soluble surfactants were tested in electrowetting systems containing lipid bilayers to see if they electrowetted reversibly.) Thus, to ensure reversible electrowetting, water drops may only contain non-fluorinated surfactants and/or electrolytes.

Furthermore, stable lipid bilayers only form on hafnium oxide surfaces out of all the dielectric surfaces tested. Other common inorganic dielectrics such as silicon dioxide and silicon nitride do not enable the formation of stable lipid bilayers. Although silicon dioxide surfaces show some tendency to form bilayers with higher concentrations of oil surfactant (~50 mM Span 85 in dodecane, for instance), the water drop still occasionally pins to a few spots on the surface during electrowetting. Hafnium oxide, by comparison, never leads to pinning, provided the concentration of oil surfactant exceeds a certain threshold.

Interestingly, platinum surfaces also become hydrophobic upon submersion in similar oil phases, indicating lipid bilayer formation, but the lipid bilayer is electrically fragile and immediate ruptures when the water drop and the platinum substrate are grounded with respect to each other, suggesting that the bilayer breaks down at voltages lower than the work function of the electrical components in the setup. Ideally, the properties of the lipid bilayer would be studied using such a platform, as it would be the only dielectric layer in such a system (platinum, which is highly conductive, would function as the electrode). However, since the lipid bilayer is too electrically fragile to be studied as the sole dielectric layer in an electrowetting system of this nature, the lipid bilayer was only studied as formed on a thin hafnium oxide dielectric. Electrical properties of the hafnium oxide film were measured independently and subtracted out from the total dielectric properties of the lipid bilayer *and* the hafnium oxide film to obtain the specific properties of the lipid bilayer.

1.4 Thesis objectives

This thesis demonstrates the first-time use of lipid bilayers as reversibly wettable organic dielectrics in electrowetting systems. As this thesis will show, lipid bilayers have the ability to produce high changes in water contact angles at exceptionally low voltages. Furthermore, this thesis aims to quantify some of the physical and electrical properties of lipid bilayers in electrowetting systems for the purposes of assessing the capabilities and the limitations of utilizing these thin liquid films in future electrowetting devices. Specifically, this thesis focuses on properties of lipid bilayers formed using sorbitan monooleate (Span 80) and sorbitan trioleate (Span 85) in dodecane. The properties measured include the thickness of the lipid bilayer with respect to electrostatic pressure applied to the water drop, leakage current through the lipid bilayer resulting from the applied electric field across the lipid bilayer, and an assessment of the lipid bilayer morphology assuming a densely-packed polymer brush model. Preliminary results on changes in lipid bilayer thickness overtime in response to a step change in voltage are also presented.

CONTACT ANGLE AS A FUNCTION OF VOLTAGE

2.1 Measuring contact angles in electrowetting systems

To characterize the electrowetting behavior of systems containing lipid bilayers, a degenerately boron doped single crystal silicon electrode coated with a thin hafnium oxide film (~9 nm) was submersed in dodecane with a dissolved surfactant, and a water drop (~3-4 mm diameter) containing electrolytes and/or surfactants was deposited onto the hafnium oxide surface, as shown in Figure 1a. A platinum electrode was brought into contact with the water drop, and a voltage was applied to the water drop while the silicon was grounded. Applied voltage in the form of an AC sinusoidal wave from V to -V at a specified frequency was incremented from 0 V to a maximum voltage (forward sweep), resulting in wetting, and then decremented back to 0 V (reverse sweep), resulting in dewetting. The water drop contact angle (θ) was recorded for each applied voltage.

All contact angle measurements were determined optically using a Ramé-Hart goniometer (example drop image depicted in Figure 3). The software DropImage Advanced was used to trace the surface of the water drop in the captured image and calculate the angle of the tangent line that the drop makes with the solid surface. The circular curve fit method was used for all contact angle measurements presented in this thesis.

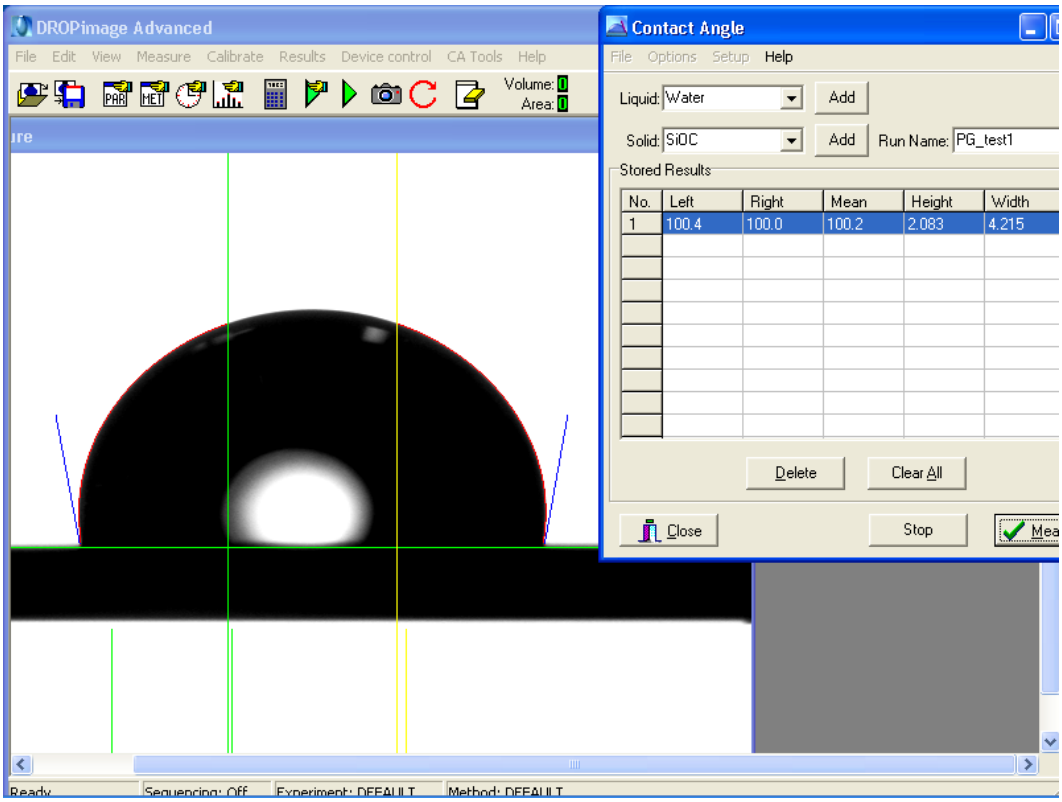

Figure 3. An example of measuring the contact angle of a liquid drop on a solid surface. The green and yellow vertical markers are placed to the left and right of the platinum electrode (not depicted here, though normally present during electrowetting experiments). The green horizontal line is aligned with the base of the liquid drop in contact with the solid surface. The goniometer software traces the surface of the drop (indicted by red arcs) and computes the tangent lines (blue) on the left and right side of the drop. As reflected in the contact angle measurement window in the upper right corner of the screen, the left and right contact angles typically measure within 1-2 degrees of each other.

2.2 Contact angle vs. voltage plots

Figure 4a shows the electrowetting behavior of two systems containing lipid bilayers. The top curve in Figure 4a corresponds to an electrowetting system that reached contact angle saturation around 115° (partial wetting system), whereas the bottom curve corresponds to an electrowetting system containing additional water surfactants that showed virtually no contact angle saturation (complete wetting system). Photographs of the complete wetting system at different voltages are provided in Figure

4b. The water surfactants used in this system are sodium decyl sulfate and sodium dodecyl sulfate, both of which consist of a negatively charged sulfate head group attached to a single saturated hydrocarbon tail. Sodium decyl sulfate and sodium dodecyl sulfate contain hydrocarbon tail lengths of 10 and 12 carbons, respectively. These surfactants significantly lower the oil-water surface tension in the presence of Span 80 and Span 85. For the purposes of electrowetting, the low oil-water surface tension decreases the minimum obtainable contact angle (i.e. saturation point) in these systems. Such low surface tensions significantly affect the Bond number, which may influence the contact angle measurements at high angles.

The Bond number (Bo) is a dimensionless quantity that compares the relative influence of surface tension forces and gravity forces on a body. In case of high Bond numbers (>~10), gravity forces dominate. In the case of low Bond numbers (<~0.1), surface tension forces are considered dominant. The Bond number is defined as follows:

$$Bo = \frac{\rho g' l^2}{\sigma} \tag{2}$$

where ρ is the density of the water drop, l is the length scale of the water drop, σ is the oil-water surface tension, and g' is the relative acceleration due to gravity, defined as:

$$g' = g\left(\frac{\rho_2 - \rho_1}{\rho_2}\right) \tag{3}$$

where g is the regular acceleration due to gravity, ρ_2 is the density of the water drop, and ρ_1 is the density of the surrounding oil. Approximating l as 1 mm, the Bond number for the water drop in these types of low-surface tension systems exceeds 10. Thus, gravity forces dominate in these systems, and the drop adopts a more "blob-like" shape as opposed to a spherical configuration. In terms of contact angle measurements, the high Bond number contributes to the distortion of the drop shape and potentially results in underestimations of the contact angle, most notably at high angles. However, at microfluidic length scales, the Bond number is significantly lower, and gravity effects are considered negligible.

(a)

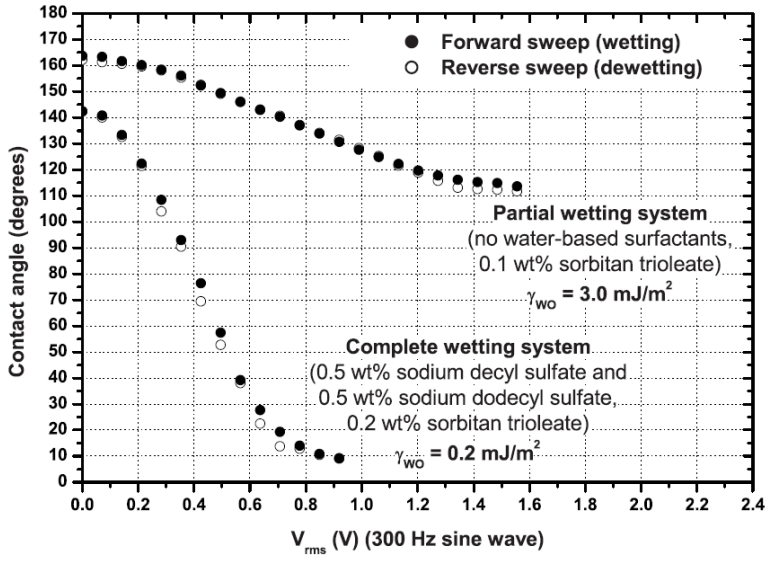

(b)

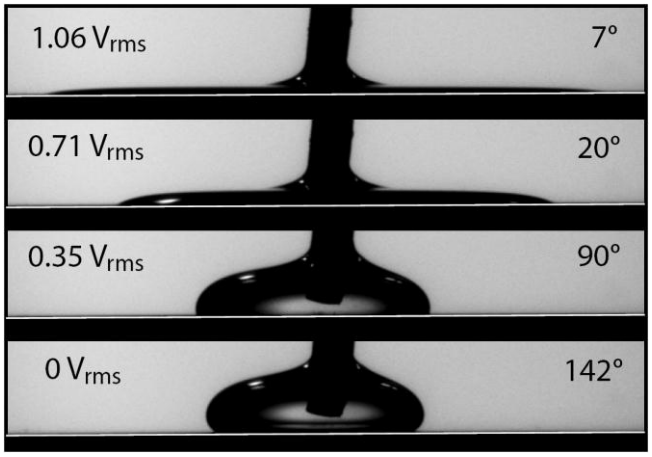

Figure 4. (a) Electrowetting behavior of two systems containing lipid bilayers. The partial wetting system contained 9 nm of hafnium oxide, a 0.1 N NaCl water drop, and dodecane with 0.1 wt. % sorbitan trioleate. The complete wetting system contained additional water surfactants (0.5 wt. % sodium decyl sulfate and 0.5 wt. % sodium dodecyl sulfate) and 0.2 wt. % sorbitan trioleate. The partial wetting system reached contact angle saturation around 115°, whereas the complete wetting system electrowetted below 10°, showing virtually no saturation. (b) Images of the complete wetting system captured as voltage decreased (from top to bottom chronologically). The contact angle fully restored to Young's angle (142°) at 0 V after the drop electrowetted to 7° at 1.06 V.

In addition to enabling high contact angle changes at low voltages, lipid bilayers formed on hafnium oxide surfaces prove remarkably stable in reliability tests. Within the time ranges tested, lipid bilayers do not break down, and they completely prevent contact between the water drop and the hafnium oxide surface, even after thousands of electrowetting cycles. An example of a reliability experiment performed with a lipid bilayer electrowetting system is presented in Figure 5. This system contained just 0.1 wt% Span 85 (around the minimum threshold required for stable bilayer formation) and was electrowetted for over 40 hours with a 75% duty cycle. The sharp initial decrease in contact angle in the wetted state reflects the lowering of the oil-water surface tension during the reliability experiment as the water drop equilibrated with the surrounding oil phase. This experiment commenced almost immediately after the water drop was dispensed onto the hafnium oxide surface in the oil phase.

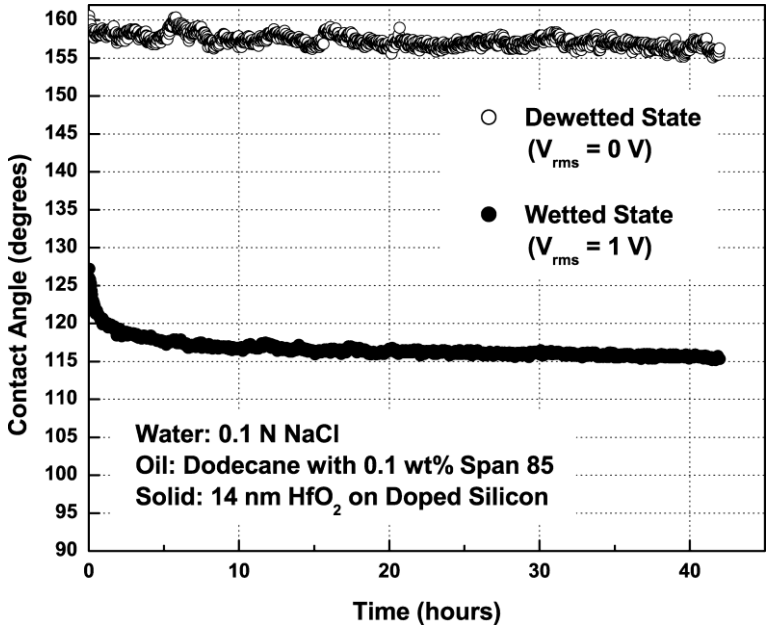

Figure 5. Reliability experiment of electrowetting system containing a lipid bilayer. The water phase contained 0.1 N NaCl, and the ambient oil phase consisted of dodecane with 0.1% Span 85. AC Voltage (peak voltage=1 V, 100 Hz, square wave) was applied in 120-second cycles with the voltage on for 90 seconds and off for 30 seconds. The contact angle was measured each cycle for both the wetted and dewetted states. The contact angles in each state for each cycle are plotted against time.

2.3 Discussion on electrowetting with lipid bilayers

As illustrated in Figure 4, electrowetting systems with lipid bilayers can produce high contact angles with very low voltages. Lipid bilayers can even produce complete wetting, which is rarely achieved in electrowetting. Moreover, electrowetting on lipid bilayers is highly predictable and reversible. The thin oil film enables completely reversible wetting; the drop shape switches consistently and seamlessly between different contact angles for different applied voltages without sticking to the surface.

Furthermore, as demonstrated in the reliability test, lipid bilayers remain stable over the course of thousands of electrowetting cycles, completely preventing the water drop and the hafnium oxide surface from coming into contact. Interestingly, the system tested here showed a slight decrease in the wetted contact angle overtime, whereas fluoropolymer-based electrowetting systems typically show a gradual increase in the wetted contact angle. The lowering of the wetted angle could be an indication of lowering oil-water surface tension over the course of the experiment. Over the course of nearly two days, a visually observable layer of surfactant slowly formed around the surface of the drop. This layer of surfactant gave the water drop a somewhat cloudy, opaque appearance. Interestingly, no cloud forms when the drop is continually electrowetted; in such instances, the drop remains optically clear as ever, even if the drop has been sitting in the oil medium for days. Only when the drop is dewetted for prolonged periods of time does the cloud of surfactant crowd the surface of the water drop. In the case of the reliability experiment, the 30-second intervals during which the drop was dewetted appear to have allowed the surfactant to gradually crowd the interface.

LIPID BILAYER THICKNESS IN RESPONSE TO ELECTROSTATIC PRESSURE

3.1 Measuring lipid bilayer thickness electrically

The lipid bilayer and the hafnium oxide film act as two capacitors in series in the electrowetting configuration, as shown in Figure 6. By measuring the capacitance per area across the lipid bilayer/hafnium oxide dielectric stack, the thickness of the lipid bilayer may be measured, provided the capacitance per area of the hafnium oxide film is known. The capacitance per area of the lipid bilayer (C_{oil}), capacitance per area of the hafnium oxide (C_{HfO_2}), and capacitance per area of the lipid bilayer/hafnium oxide stack (C_{total}) are related as follows:

$$\frac{1}{C_{total}} = \frac{1}{C_{HfO_2}} + \frac{1}{C_{oil}} \qquad \text{or} \qquad C_{oil} = \frac{1}{\frac{1}{C_{total}} - \frac{1}{C_{HfO_2}}} \tag{4}$$

In these experiments, C_{total} and C_{HfO_2} were measured directly by applying a sinusoidal voltage across the lipid bilayer/hafnium oxide stack in the electrowetting system and across the hafnium oxide dielectric in air, respectively, at different voltages. C_{oil} was then calculated for the different applied voltages using Equation 4, and the effective thickness of the lipid bilayer (t_{oil}) at each voltage was determined using the following relation:

$$t_{oil} = \frac{\varepsilon_0 \varepsilon_{oil}}{C_{oil}} \tag{5}$$

where ε_0 is the permittivity of vacuum and ε_{oil} is the relative permittivity of the lipid bilayer. For these calculations, ε_{oil} was taken to be the relative permittivity of dodecane, as dodecane was used for all the oil phases in these experiments and the addition of small concentrations of surfactant to the oil (~1% by weight) should not significantly change the relative permittivity of the oil.

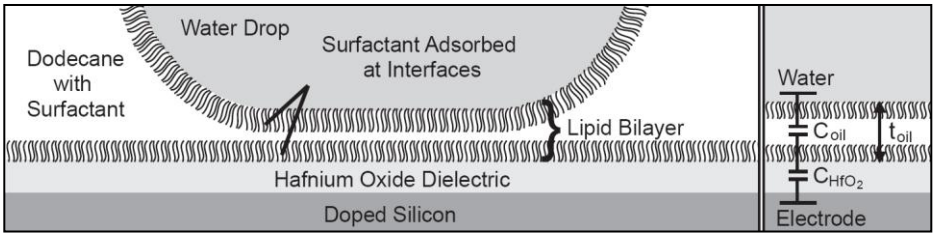

Figure 6. Electrical schematic of the lipid bilayer. Electrically, the lipid bilayer functions as a capacitor in series with the hafnium oxide film. Both dielectric layers are between the water drop and the doped silicon substrate. In the low frequency ranges tested (~100-300 Hz), the water drop and the silicon substrate function as conductors.

The electrostatic pressure (P_{elec}) exerted on the water drop during electrowetting may be calculated using C_{oil}, C_{HfO_2}, and V, or alternatively C_{total} and V, with either of the following electrically equivalent formulas:

$$P_{elec} = \frac{1}{2\varepsilon_0\varepsilon_{oil}}\left(\frac{C_{oil}C_{HfO_2}V}{C_{oil}+C_{HfO_2}}\right)^2, \tag{6}$$

$$\text{or equivalently,} \quad P_{elec} = \frac{1}{2\varepsilon_0\varepsilon_{oil}}(C_{total}V)^2 \tag{7}$$

Thus, the lipid bilayer thickness and the electrostatic pressure exerted on the water drop may be calculated for a given voltage, and a relation between the bilayer thickness and the electrostatic pressure may be obtained.

The voltage drop across the lipid bilayer (V_{oil}) may also be calculated for a given applied voltage if C_{HfO_2} and C_{oil} are both known. V_{oil} is calculated as follows:

$$V_{oil} = V\left(\frac{C_{HfO_2}}{C_{HfO_2}+C_{oil}}\right) \tag{8}$$

In this way, a relationship between t_{oil} and V_{oil} may be obtained.

3.2 Experimental setup for measuring lipid bilayer thickness

The experimental setup used to measure contact angles proved insufficient for precise measurement of the lipid bilayer thickness; the oil surfactant molecules readily coated the platinum electrode, potentially creating a voltage drop across the electrode/water interface. In a system with such a thin capacitive layer, it became necessary to remove the platinum electrode, and simply sandwich the water drop in between two identical hafnium oxide surfaces in oil. In this configuration, the only capacitive layers were two identical lipid bilayer/hafnium oxide dielectric stacks. The measured capacitance for this configuration must be multiplied by a factor of two to obtain the capacitance value for a single hafnium oxide/lipid bilayer stack.

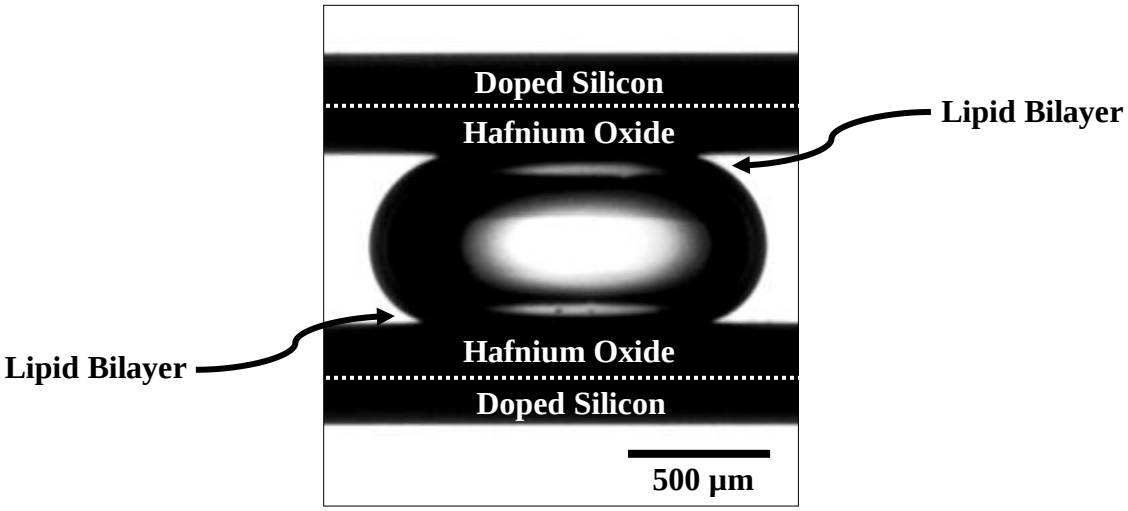

Figure 7. Experimental configuration used to measure lipid bilayer thickness for different applied voltages. A water drop was dispensed in the oil phase between two identical parallel electrodes coated with a thin hafnium oxide layer, and the resulting capacitance was measured. The layers depicted in this figure are not to scale.

The capacitance measurements that were used to calculate the lipid bilayer thickness were measured using an Agilent 4284A (20 Hz-1 MHz) Precision LCR meter. The series resistance and

capacitance of the water drop as well as the base area of the drop were recorded in the electrowetting system (with the lipid bilayer), and the corresponding measurements were recorded in air (without the lipid bilayer). AC voltage (100 Hz, sinusoidal) was used for these experiments.

3.3 Lipid bilayer thickness measurements

The thicknesses of lipid bilayers formed from 10 mM Span 80 and 10 mM Span 85 in dodecane were measured electrically for different applied AC voltages (100 Hz, sinusoidal). Figure 8a plots the lipid bilayer thickness versus voltage applied to the system. Figure 8b shows the lipid bilayer thickness as a function of the voltage drop across only the lipid bilayer. In the case of both surfactants, the lipid bilayer thickness decreases as the applied voltage increases, indicating a thinning of the lipid bilayer as the drop is electrowetted.

Figure 9 shows the electrostatic pressure applied to the drop as the drop is electrowetted as a function of the lipid bilayer thickness. As the drop is electrowetted with increasing voltage, the electrostatic pressure exerted on the drop increases, and the lipid bilayer thins.

(a)

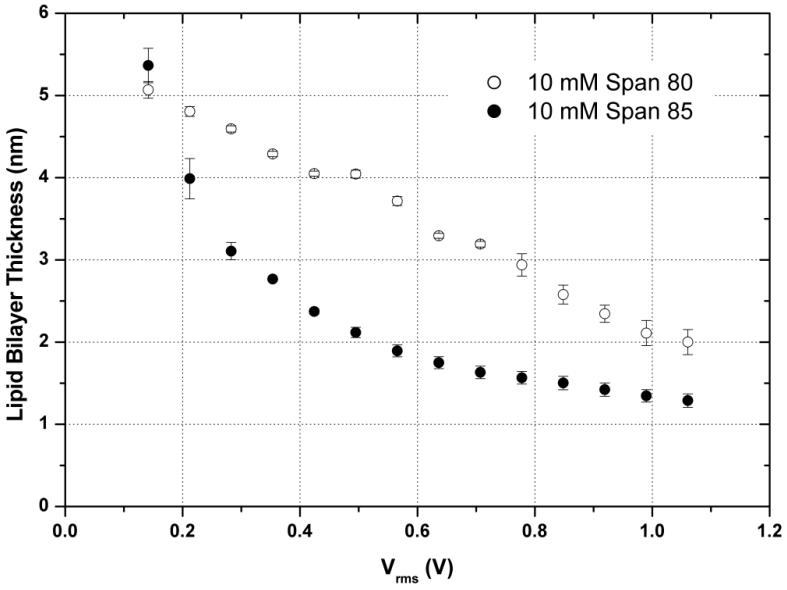

(b)

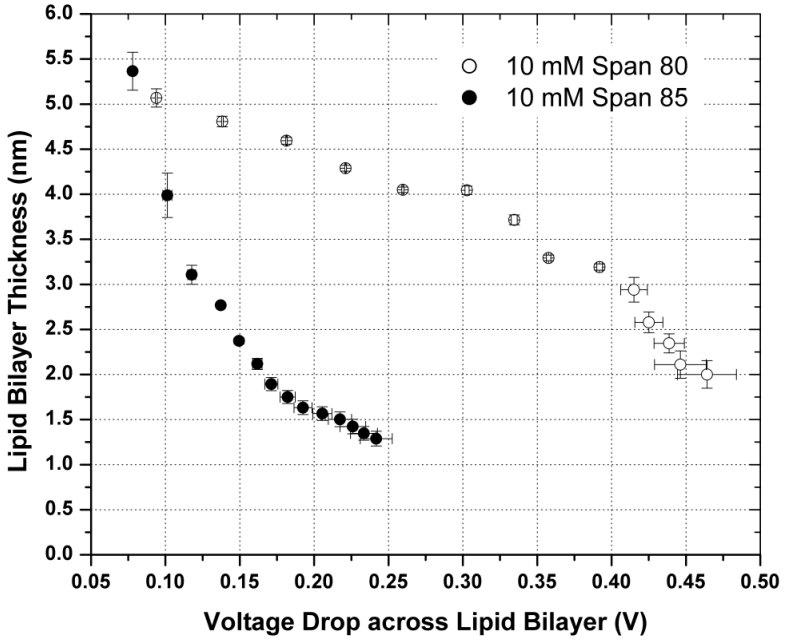

Figure 8. (a) Lipid bilayer thickness as a function of voltage applied across the lipid bilayer/hafnium oxide stack for 10 mM of Span 80 and Span 85. Span 85 forms a thinner lipid bilayer than Span 80 with respect to voltage. (b) Lipid bilayer thickness vs. voltage drop across the lipid bilayer. Span 85 forms a thinner lipid bilayer with respect to the voltage drop across the lipid bilayer than does Span 80. In both plots, error bars correspond to ± one standard deviation from the mean measurement (plotted), calculated from three experimental runs for each surfactant.

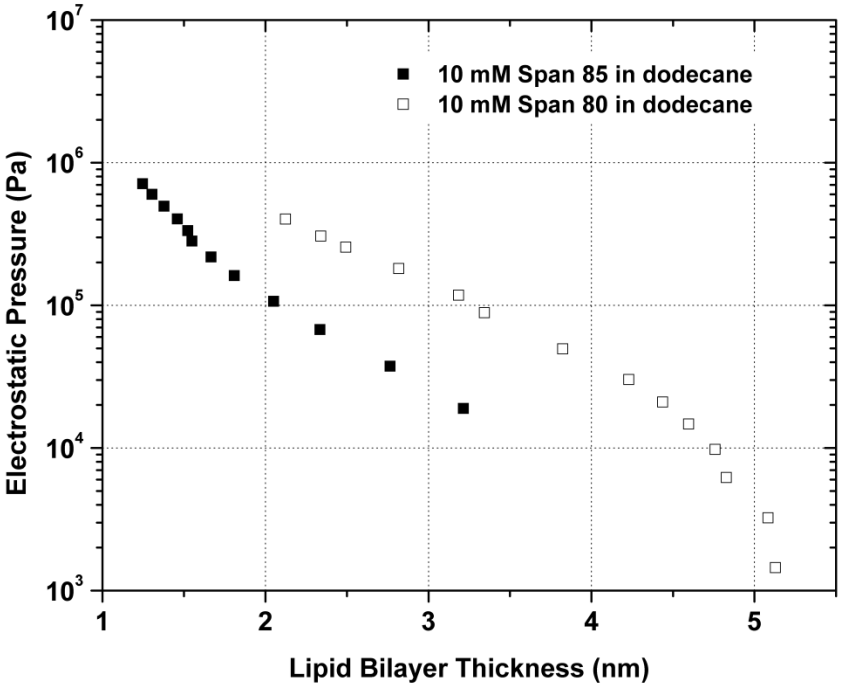

Figure 9. Electrostatic pressure vs. lipid bilayer thickness for lipid bilayers formed with 10 mM Span 80 and Span 85 in dodecane. As the drop is electrowetted, the electrostatic pressure increases and the lipid bilayer compresses.

3.3 Discussion on the measured lipid bilayer thicknesses

The measured thicknesses for the lipid bilayers reveal that Span 85 forms a thinner lipid bilayer at identical concentrations and voltages than does Span 80. Span 80 forms a thicker lipid bilayer, even for identical voltage drops across the lipid bilayer. The thicker separation between the two layers of the bilayer in the case of Span 80 may be attributed to the structural differences between Span 80 and Span 85. Individual Span 80 molecules may have the ability to adopt a more densely packed configuration on the oil-water and oil-hafnium oxide interfaces, as each molecule only contains one lipid tail. A higher concentration of molecules along the surface may lead to a thicker lipid bilayer, due to more crowding of surfactant molecules along the interface.

CHARACTERIZING LIPID BILAYER MORPHOLOGY

4.1 Theoretical model for disjoining pressure of a polymer brush

The equilibrium thickness of the lipid bilayer is governed by a balance between the electrostatic pressure exerted on the water drop during electrowetting (P_{elec}) and the disjoining pressure arising from the repulsion between the adsorbed surfactant molecules (P_{brush}), assuming a negligible hydrostatic pressure. For the size drops used in these experiments, the hydrostatic pressure was 2-3 orders of magnitude smaller than both the electrostatic and the disjoining pressures, rendering its effect insignificant for the purposes of these calculations. When the drop is electrowetted, P_{elec} pushes the water drop towards the hafnium oxide surface, whereas P_{brush} repels the water drop from the hafnium oxide surface. If the lipid bilayer is modeled as a densely packed polymer brush, P_{brush} may be calculated in terms of t_{oil} as follows [23]:

$$P_{brush} = k_B T \Gamma^{3/2} \left[\left(\frac{2h_0}{t_{oil}} \right)^{9/4} - \left(\frac{t_{oil}}{2h_0} \right)^{3/4} \right] \tag{8}$$

where Γ is the surface density of surfactant molecules and h_0 is the height of the polymer brush. Once a relationship between P_{elec} versus t_{oil} is obtained, P_{brush} may be aligned with the values of P_{elec} over the range of measured values for t_{oil} obtained during electrowetting using two fitting parameters: Γ and h_0. Thus, the surface density of surfactant molecules and the polymer brush height may be estimated in lipid bilayers formed from a given surfactant at a given concentration. See Appendix B for an explanation of this equation. (A partial derivation may also be found in [23].)

4.2 Plots of bilayer thickness vs. electrostatic and disjoining pressures

Pressure versus lipid bilayer thickness is plotted in Figure 10 for equal molar concentrations of Span 80 and and Span 85 in dodecane. Theoretical calculations of the disjoining

pressures arising in these lipid bilayers are overlapped with the measured electrostatic pressures. The values for Γ and h_0 used to calculate the theoretical disjoining pressure curves are provided in Figure 9. These values were obtained by aligning the theoretical disjoining pressure curves with the measured electrostatic data points.

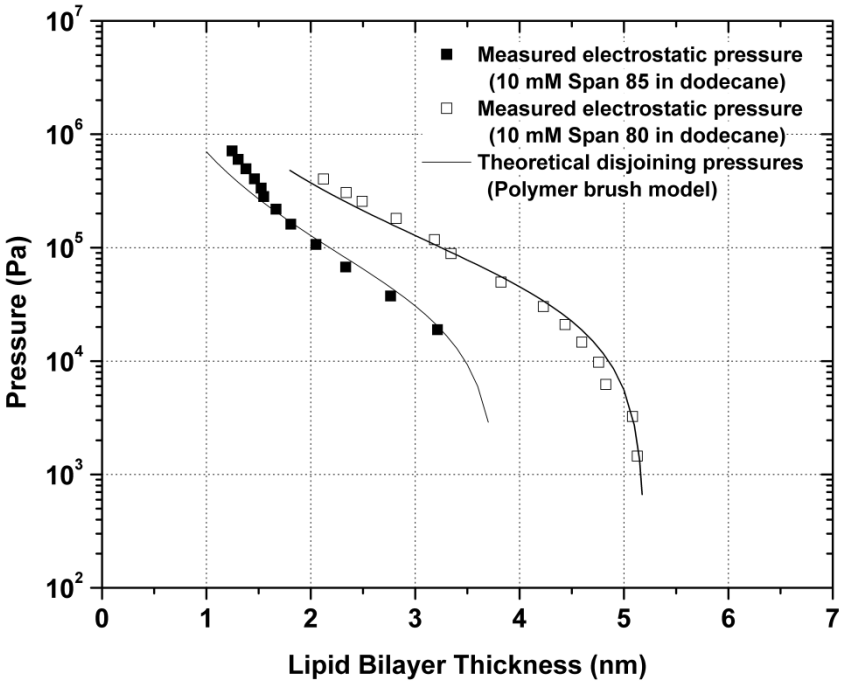

Figure 10. Measured electrostatic pressures and theoretical disjoining pressures for lipid bilayers formed from 10 mM Span 80 and 10 mM Span 85 in dodecane. Values for the two fitting parameters Γ and h_0 are provided for each surfactant in Table 2.

Table 2. Values for Γ and h_0 used to calculate the P_{brush} curves displayed in Figure 9.

	Γ (molecules/m^2)	h_0 (nm)
Span 80	**5.0×10^{16}**	**2.6**
Span 85	**4.2×10^{16}**	**1.9**

4.3 Discussion of lipid bilayer morphology

The values for the fitting parameters Γ and h_0 used to calculate the disjoining pressures depicted in Figure 9 are provided in Table 2. The h_0 values for these surfactants are roughly within the range of the chain lengths for these molecules. However, the predicted chain length for Span 85 is larger than the chain length for Span 80, given that Span 85 contains 3 lipid tails and Span 80 only contains 1. The thinner lipid bilayer resulting from Span 85 may reflect a different packing conformation of Span 85 along the oil-water and oil-hafnium oxide interfaces that comprise the lipid bilayer. For instance, Span 85 may pack less densely on the surface (as also supported by the lower Γ value) such that the molecules are more spread apart and more folded. In the case of Span 80, the tighter packing of molecules may lead to a more upright configuration of Span 80 molecules packed along the surface.

The close alignment between the calculated disjoining pressures and the measured electrostatic pressures for both surfactants supports the observation that these lipid bilayers can be modeled as densely packed polymer brushes. The curves for Span 85 show some deviation at high electric fields; as the lipid bilayer approaches ~1 nm thickness, the disjoining pressure according to the polymer brush model deviates from the measured electrostatic pressure. At these thicknesses, there may be other mechanisms of repulsion between the water drop and the hafnium oxide surface.

LEAKAGE CURRENT THROUGH THE LIPID BILAYER UNDER ELECTRIC FIELD

5.1 Electrical model of the lipid bilayer

Interestingly, the electrowetting effect only works in systems containing lipid bilayers with AC voltages at frequencies around 50 Hz and above. In the case of lower frequency AC voltages or DC voltages, electrowetting is completely ineffective in systems with lipid bilayers, producing no lasting change in contact angle. Under low-frequency AC square wave voltages, water drops in lipid bilayer systems exhibit a decrease in contact angle with each half-cycle, immediately followed by a spontaneous increase in contact angle. Thus the electrowetting effect is only sustainable for small timescales. This observation suggests that the lipid bilayer does not function as an ideal dielectric but rather leaks charge, presumably on timescales around 50 Hz. It stands to reason that in the case of higher frequency AC voltages, the constant switching of charge polarity does not allow sufficient time for the lipid bilayer to leak charge within an AC voltage half-cycle, and so the drop remains electrowetted as long as the AC voltage is applied. Further characterization of the leakage current through the lipid bilayer in response to applied voltage is presented in subsequent sections.

As evidenced by the inability of lipid bilayers to enable electrowetting with voltage waveforms at frequencies below 50 Hz, the lipid bilayer exhibits some tendency to leak charge when a voltage is applied across the layer. This electrical behavior suggests that the lipid bilayer exhibits both capacitive and resistive characteristics during electrowetting. Especially at low frequencies, the resistive behavior of the lipid bilayer becomes apparent. Indeed, the current response of the electrowetting system when subject to an AC square wave voltage exhibits behavior that deviates from that of a pure capacitor. As in the case of a capacitor, the current response shows a clear spike in current each time the voltage switches polarity. However, unlike the case of a pure capacitor, the electrowetting system displays a distinct residual current following the characteristic current spike in current each time the voltage switches polarity, depicted in Figure 11.

Although the lipid bilayer displays both capacitive and resistive tendencies, preliminary measurements indicated that the lipid bilayer cannot be accurately modeled as a linear capacitor and a linear resistor in parallel. In particular, the resistance of the lipid bilayer is electric field-dependent, rendering conventional methods of measuring the lipid bilayer resistivity (e.g. using an LCR meter) ineffective.

5.2 Measuring leakage current through the lipid bilayer

In these experiments, the leakage current across the oil layer was obtained in response to electric field strength from the measured current response to an AC square wave voltage. By visually inspecting the current response of the electrowetting system, it is apparent that a residual current appears following a pronounced current spike. This current spike, which is distinctive to a capacitor-based system, corresponds to the charging of the system capacitor (here, the hafnium oxide and lipid bilayer thin films in series). The residual current following the current spike corresponds to the current that leaks through the lipid bilayer after the system capacitor (i.e. the hafnium oxide and lipid bilayer in series) has fully charged. In a system with a pure capacitor that does not leak a significant amount of charge, there is no current (or "tail") that follows after the voltage spike. Thus, the leakage current through the oil layer may be approximated as the current at the point at which the tail begins.

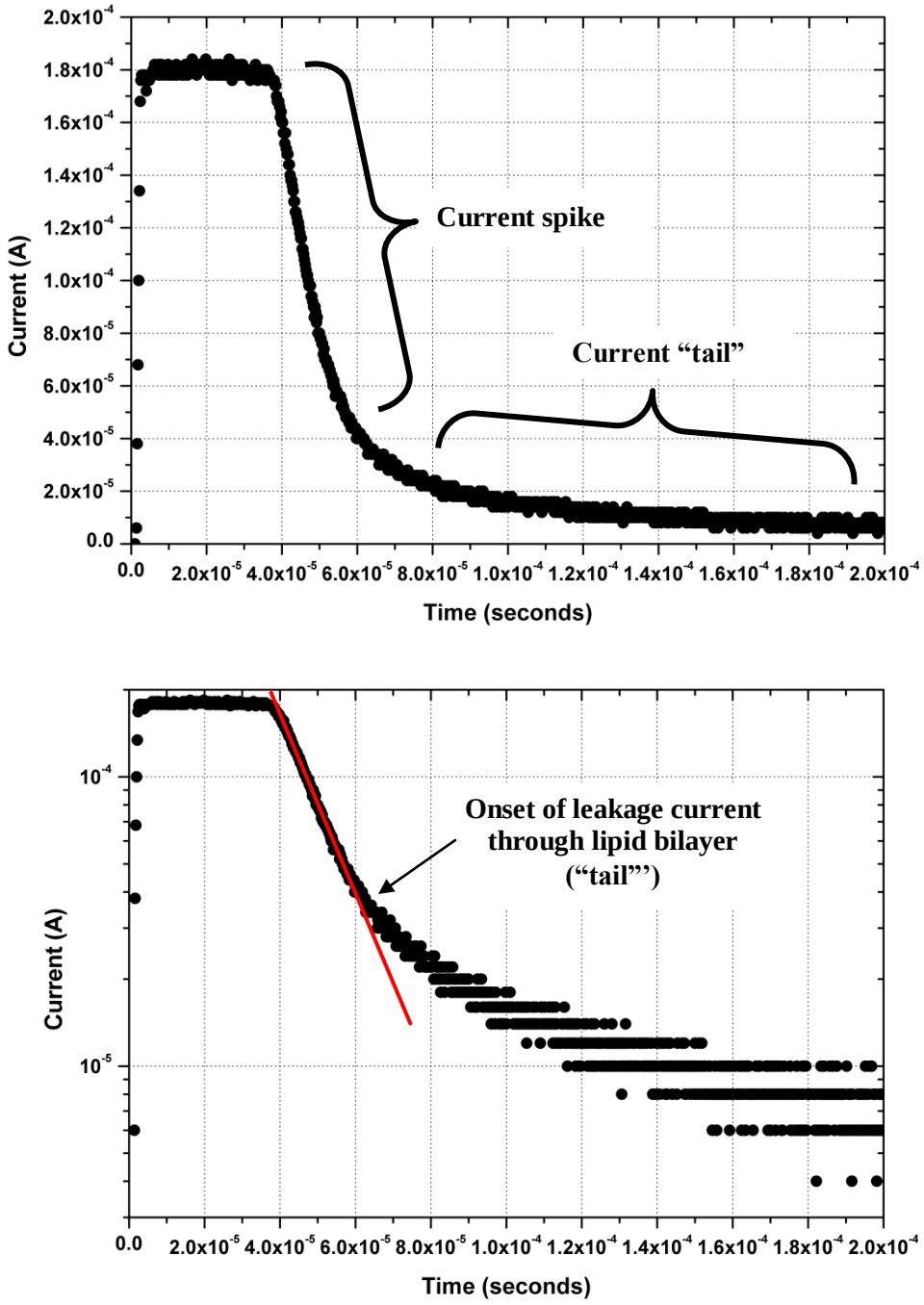

Figure 11. Representative current response of an electrowetting system containing a lipid bilayer when actuated with an AC square wave voltage. The current shows a characteristic "tail" following the voltage spike triggered by the change in polarity of the square wave. This behavior is not seen in systems without lipid bilayers. The saturation of the voltage spike around 1.8×10^{-4} A is caused by the voltage source used to power the measurement setup and does not reflect any characteristic behavior or property of the electrowetting system.

5.3 Calculating electric field across the lipid bilayer

The voltage across the oil layer (V_{oil}) at the point prior to leakage is simply given by the formula for a voltage divider across two capacitors in series:

$$V_{oil} = V_{rms}\left(\frac{C_{HfO_2}}{C_{oil}+C_{HfO_2}}\right) \tag{9}$$

This method assumes that the lipid bilayer is fully charged when it starts to leak charge. The electric field across the bilayer (E_{oil}) may then be obtained by dividing V_{oil} by t_{oil}:

$$E_{oil} = \frac{V_{oil}}{t_{oil}} \tag{10}$$

Thus a relationship between the leakage current across the lipid bilayer and the voltage drop across the lipid bilayer may be obtained.

5.4 Leakage current vs. electric field plots

The conductivities of lipid bilayers formed from equal molar concentrations of Span 80 and Span 85 in dodecane under a range of applied electric fields are compared in Figure 11. Span 85 shows higher leakage current through the oil layer at smaller electric fields. Thus, the addition of Span 80 does not affect the conductivity of dodecane as much as Span 85 does.

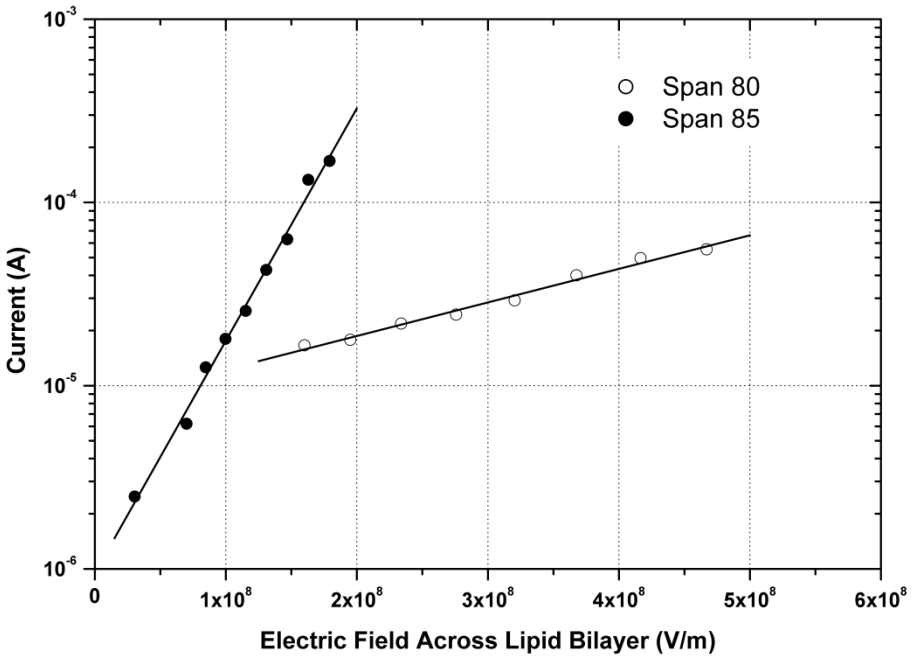

Figure 12. Leakage current across the lipid bilayer as a function of the electric field across the lipid bilayer. The oil phases consisted of dodecane with 10 mM Span 85 and 10 mM Span 80. The leakage current increases exponentially with electric field. Span 85 increases the electrical conductivity of dodecane more than Span 80.

5.5 Discussion of non-linear electrical behavior of the lipid bilayer

Lipid bilayers formed from 10 mM Span 80 and 10 mM Span 85 in dodecane both behave non-linearly in terms of electrical conductivity. Interestingly, the electrical conductivities of both these thin liquid films increase exponentially with electric field, as opposed to the linear dependence exhibited by most dielectric films. The method for charge conduction within the lipid bilayer is still not well-understood, but the non-linear behavior may be attributed in part to the changing thickness of the lipid bilayer during voltage application. Unlike solid dielectrics, liquid dielectrics change in thickness when subjected to a strong electric field. The thinning of the lipid bilayer may allow for charge to conduct more effectively across the oil-based nanoscale layers in a non-linear fashion. For electrowetting purposes, the oil phase should exhibit minimal leakage current. As seen in Figure 12, Span 80 leaks less current than Span 85 under the same electric fields and thus may work better for electrowetting applications.

TRANSIENT BILAYER THICKNESSES DURING VOLTAGE TRANSITIONS

6.1 Measuring changes in lipid bilayer thickness with time

Series capacitance and resistance values were collected every 3 seconds for several minutes as the lipid bilayer transitioned from one equilibrium height to another in response to a step change in peak voltage at time 0. AC voltages (100 Hz, sinusoidal) were used for these experiments; the peak voltage alternated between 0.5 V and 1.0 V.

6.2 Theoretical predictions for changes in lipid bilayer thickness with time

As discussed previously, the thickness of the lipid bilayer changes with applied voltage. The predicted rate of the change of the lipid bilayer thickness with respect to time is given by the following equation (see Appendix B for a full derivation):

$$\frac{dh}{dt} = \frac{2h^3}{\mu D^2}\left[\frac{1}{2\varepsilon_0\varepsilon_{oil}}\left(\frac{\frac{\varepsilon_0\varepsilon_{oil}}{h}C_{HfO_2}V}{\frac{\varepsilon_0\varepsilon_{oil}}{h}+C_{HfO_2}}\right)^2 - k_B T\Gamma^{\frac{3}{2}}\left[\left(\frac{2\mathrm{L}_0}{h}\right)^{\frac{9}{4}} - \left(\frac{h}{2\mathrm{L}_0}\right)^{\frac{3}{4}}\right]\right] \quad (11)$$

where h is the height (thickness) of the lipid bilayer, D is the diameter of the base of the water drop, μ is the viscosity of the fluid, and all other parameters are the same as defined previously. Comparing equation 11 to equations 6 and 8, it is apparent that the rate of the change of the lipid bilayer thickness with respect to time is proportional to the difference between the electrostatic and disjoining pressures. Thus, the greater the imbalance between the electrostatic and disjoining pressures, the greater the rate of change of the lipid bilayer thickness with respect to time.

6.3 Plots of lipid bilayer thickness vs. time

In an effort to understand the transient effects during wetting and dewetting transitions of the water drop, the lipid bilayer thickness was measured over the course of several minutes after a step change in peak voltage for 10 mM Span 80 in dodecane. These experiments were performed at a lower frequency than the other experiments (20 Hz, sinusoidal), and Span 85 proved too conductive to obtain steady wetting at this frequency. Figure 13 plots the lipid bilayer thickness during two runs, each containing a wetting and dewetting transition between 0.5 V and 1.0 V (peak voltages).

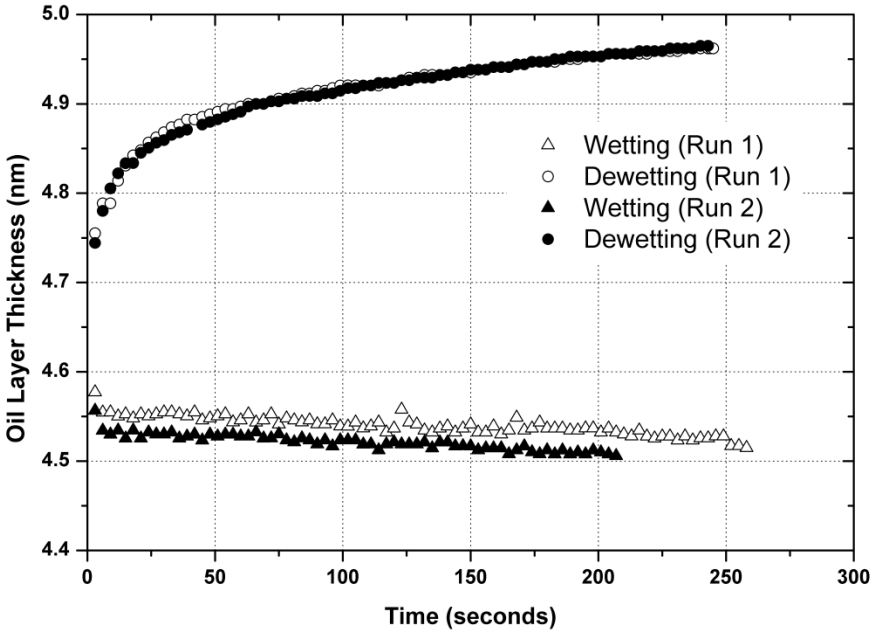

Figure 13. Evolution of lipid bilayer thickness in response to a step change in peak voltage (20 Hz, sinusoidal) during two consecutive experimental runs. Each run consists of a wetting and a dewetting transition. (Wetting transitions correspond to a peak voltage change from 0.5 V to 1 V at time 0; dewetting transitions correspond to a peak voltage change from 1 V to 0.5 V at time 0.) The dewetting transitions reveal a roughly logarithmic behavior, whereas the wetting transitions show a roughly linear behavior.

6.4 Discussion on transient lipid bilayer thicknesses

The changes in lipid bilayer thickness with time in response to step voltage changes appears to depend on the interactions of molecules within the polymer brush rather than the hydrodynamic effects of squeezing a thin liquid film. The changes in thickness overtime do not occur on the time scales expected for the hydrodynamic effects associated with squeezing a thin liquid film; rather, the adjustment of the lipid bilayer thickness with time appears to be limited by the interactions between the adsorbed molecules comprising the lipid bilayer.

The wetting and dewetting runs show distinctly different trends; the wetting transition reveals a roughly linear thickness decrease with time, whereas the dewetting transition shows a thickness dependence that is logarithmic with time. As seen in Figure 13, the lipid bilayer approaches its equilibrium height in a slower fashion during the wetting transition than during the dewetting transition, suggesting an asymmetry in the mechanism of molecular interactions between the adsorbed molecules comprising the lipid bilayer during compression and during retraction.

CONCLUSION

This thesis demonstrated the first-time use of lipid bilayers as reversibly wettable dielectrics in electrowetting systems and presented findings on various physical and electrical properties of lipid bilayers formed from Span 80 (sorbitan monooleate) and Span 85 (sorbitan trioleate) in electrowetting systems. Lipid bilayers formed from these surfactants offer several advantages over traditional hydrophobic dielectric coatings in electrowetting systems (e.g. spin-coated amorphous fluoropolymers), most notably the ability to produce high contact angle changes with exceptionally low voltages (<1-2 V), on par with electrocapillary effects observed in mercury-based systems without dielectric layers. In addition to the low-voltage capabilities, electrowetting systems containing lipid bilayers were shown to exhibit remarkably high changes in contact angle—exceeding 130° under certain conditions. Reliability experiments demonstrated that lipid bilayers are very stable overtime; no decrease in contact angle range or inconsistency in contact angle measurement was observed during more than one thousand electrowetting cycles. Electrical measurements revealed a decreasing thickness in the lipid bilayer as the applied voltage increased. By comparing the experimentally measured electrostatic pressure exerted on the drop during electrowetting to the theoretical disjoining pressure arising from a densely-packed polymer brush, the packing density of surfactant molecules as well as the height of the uncondensed polymer brush was determined for both Span 80 and Span 85. The dependence of charge-leakage on electric field for these lipid bilayers was also studied; an exponential increase in charge leakage was found with increasing electric field.

BIBLIOGRAPHY

[1] F. Mugele and J. Baret, J. Phys.: Condens. Matter 17, R705 (2005).

[2] A. Quinn, R. Sedev, and J. Ralston, J. Phys. Chem. B 109, 6268 (2005).

[3] C. W. Monroe, L. I. Daikhin, M. Urbakh, and A. A. Kornyshev, Phys. Rev. Lett. 97, 136102 (2006).

[4] A. Drygiannakis, A. G. Papathanasiou, and A. G. Boudouvis, Langmuir 25, 147 (2009).

[5] J. Heikenfeld, K. Zhou, E. Kreit, B. Raj, S. Yang, B. Sun, A. Milarcik, L. Clapp, and R. Schwartz, Nature Photon. 3, 292 (2009).

[6] R. A. Hayes and B. J. Feenstra, Nature 425, 383 (2003).

[7] H. You and A. J. Steckl, Appl. Phys. Lett. 97, 023514 (2010).

[8] S. Kuiper and B. H. W. Hendriks, Appl. Phys. Lett. 85, 1128 (2004).

[9] B. Berge and P. Peseux, Eur. Phys. J. E 3, 159 (2000).

[10] N. Binh-Khiem, K. Matsumoto, and I. Shinoyama, Appl. Phys. Lett. 93, 124101 (2008).

[11] S. S. Ramakrishna, A. E. Eckhardt, V. Srinivasan, M. G. Pollack, S. Palanki, and V. K. Pamula, Lab Chip 8, 2188 (2008).

[12] V. Schaller, A. Sanz-Velasco, A. Kalabukhov, J. F. Schneiderman, F. O¨ isjo¨en, A. Jesorka, A. P. Astalan, A. Krozer, C. Rusu, P. Enoksson, and D. Winkler, Lab Chip 9, 3433 (2009).

[13] M. Vallet, M. Vallade, and B. Berge, Eur. Phys. J. B 11, 583 (1999).

[14] J. Kedzierski, S. Berry, and B. Abedian. J. Microelectromech. Syst. 18, 845 (2009).

[15] M. Paneru, C. Priest, R. Sedev, and J. Ralston, J. Phys. Chem. C 114, 8383 (2010).

[16] B. Raj, M. Dhindsa, N. R. Smith, R. Laughlin, and J. Heikenfeld, Langmuir 25, 12387 (2009).

[17] J. Kedzierski and S. Berry, Langmuir 22, 5690 (2006).

[18] H. Moon, S. K. Cho, R. Garrell, and C. J. Kim, J. Appl. Phys. 92, 4080 (2002).

[19] N. Ivosevic and V. Zutic, Langmuir 14, 231 (1998).

[20] F. Gao, Z. G. Su, P. Wang, and G. H. Ma, Langmuir 25, 3832 (2009).

[21] L. H. Princen, J. A. Stolp, and R. Zgol, J. Colloid Interface Sci. 28, 466 (1968).

[22] S. Punnamaraju and A. J. Steckl, Langmuir 27(2), 618 (2011).

[23] Chemical structures and molecular weights obtained from www.sigma-aldrich.com.

[24] P. G. de Gennes, Adv. Colloid Interface Sci. 27, 189 (1987).

APPENDIX A

Table of Constants

Constant	Name	Value	Units
ρ_{water}	Density of water	1.00	g/mL
$\rho_{dodecane}$	Density of dodecane	0.75	g/mL
g	Gravity acceleration	9.8	m/s^2
ε_0	Permittivity of vacuum	8.85×10^{-12}	F/m
ε_{oil}	Relative permittivity of oil	2.1	[ ]
k_B	Boltzmann constant	1.38×10^{-23}	J/K

APPENDIX B

Explanation of the theoretical disjoining pressure for a densely packed polymer brush:

First, the adsorbed surfactant molecules in the polymer brush are assumed to have a "self-similar" packing density, meaning that the spacing between adjacent surfactant molecules is assumed to equal the distance from the surface at which the molecules are adsorbed. Thus, the spacing between adjacent molecules at the center of the polymer brush is taken to be h_0.

$$P_{brush} = k_B T \Gamma^{3/2} \left[\left(\frac{2h_0}{t_{oil}} \right)^{9/4} - \left(\frac{t_{oil}}{2h_0} \right)^{3/4} \right]$$

In the case of a compressed polymer brush, there are two forces: the osmotic pressure in the compressed lipid bilayer, and an elastic restoring force that occurs between the two layers in close proximity. The first term in the disjoining pressure equation corresponds to the osmotic pressure term; the second term corresponds to the elastic restoring force. The osmotic term assumes no change in the density of surfactant molecules during the compression.

Deriving the rate of change of lipid bilayer thickness with respect to time:

Total volume of lipid bilayer beneath water drop:

$$V = \frac{\pi D^2}{4} h$$

Differentiating volume with respect to time:

$$\frac{dV}{dt} = \frac{\pi D^2}{4} \frac{dh}{dt}$$

Solving for the average flow velocity:

$$\frac{dV}{dt} + \pi D \bar{u} = 0$$

$$\bar{u} = -\frac{D \frac{dh}{dt}}{4h} = -\frac{R \frac{dh}{dt}}{2h}$$

Flow profile:

$$u(y) = \frac{1}{2\mu} \frac{dP}{dx} (H^2 - y^2)$$

Average flow velocity:

$$\bar{u} = \frac{1}{H} \int_0^H u(y) dy = -\frac{1}{3} \frac{dP}{dx} \frac{H^2}{\mu} = -\frac{1}{12} \frac{dP}{dx} \frac{h^2}{\mu}$$

Pressure as a function of radius:

$$\frac{dP}{dr} = \frac{12\mu\bar{u}}{h^2}$$

$$P(r) = \frac{12\mu\bar{u}(R - r)}{h^2}$$

Solving for the total force exerted on the drop:

$$F = \int_0^R P(r) \cdot 2\pi r dr = \frac{24\pi\mu\bar{u}}{h^2} \cdot \int_0^R (R - r) r dr = \frac{4\pi\mu\bar{u}}{h^2} R^3$$

Dividing the force by the area yields the average pressure, which equals the difference between the disjoining pressure and the electrostatic pressure:

$$\bar{P_v} = \frac{F}{\pi r^2} = \frac{4\pi\mu\bar{u}R}{h^2} = \frac{4\pi\mu R}{h^2} \cdot \frac{R\frac{dh}{dt}}{2h} = \frac{2\mu R^2 \frac{dh}{dt}}{h^3} = \frac{\mu D^2 \frac{dh}{dt}}{2h^3} = P_E - \pi(h)$$

Solving for dh/dt:

$$\frac{dh}{dt} = \frac{2h^3}{\mu D^2}[P_E - \pi(h)]$$

Equations for the disjoining pressure and electrostatic pressure:

$$\pi(h) = k_B T \Gamma^{\frac{3}{2}} \left[\left(\frac{2\mathrm{L}_0}{h} \right)^{\frac{9}{4}} - \left(\frac{h}{2\mathrm{L}_0} \right)^{\frac{3}{4}} \right]$$

$$P_E(h) = \frac{1}{2\varepsilon_0 \varepsilon_{oil}} \left(\frac{\frac{\varepsilon_0 \varepsilon_{oil}}{h} C_{HfO_2} V}{\frac{\varepsilon_0 \varepsilon_{oil}}{h} + C_{HfO_2}} \right)^2$$

Final equation for dh/dt:

$$\frac{dh}{dt} = \frac{2h^3}{\mu D^2} \left[\frac{1}{2\varepsilon_0 \varepsilon_{oil}} \left(\frac{\frac{\varepsilon_0 \varepsilon_{oil}}{h} C_{HfO_2} V}{\frac{\varepsilon_0 \varepsilon_{oil}}{h} + C_{HfO_2}} \right)^2 - k_B T \Gamma^{\frac{3}{2}} \left[\left(\frac{2\mathrm{L}_0}{h} \right)^{\frac{9}{4}} - \left(\frac{h}{2\mathrm{L}_0} \right)^{\frac{3}{4}} \right] \right]$$